

ACHIEVEMENT OF ROTORCRAFT HANDLING QUALITIES SPECIFICATIONS VIA FEEDBACK CONTROL

William L. Garrard, Eicher Low, Peter A. Bidian

Department of Aerospace Engineering and Mechanics
University of Minnesota
Minneapolis, USA

Abstract

A methodology for the design of control laws for augmentation of helicopter handling qualities is presented. This procedure uses eigenstructure assignment techniques to design inner loop control laws which decouple roll, pitch and yaw rates and vertical velocity, provide appropriate bandwidths in all channels, and stabilize low frequency open loop instabilities. Various response types can be easily realized by simple single loop feedbacks and feedforwards wrapped around these inner loops. Both time and frequency responses show that the closed loop helicopter provides excellent nominal performance in terms of insensitivity to gusts, tracking of pilot commands and achievement of desired response type characteristics (handling qualities). Stability robustness was investigated by approximating unmodeled rotor dynamics, actuators, sensors, filters, sampling and computational delays, etc. by a single time delay. The effect of this uncertainty on the system was evaluated using unstructured singular value techniques. The effects of variations in aerodynamic stability and control coefficients was evaluated by the stochastic root locus.

Nomenclature

Scalars

i	= $\sqrt{-1}$
s	= Laplace operator
u	= forward velocity, ft./sec
v	= lateral velocity, ft./sec
w	= vertical velocity, ft./sec
p	= roll rate, rad/sec
q	= pitch rate, rad/sec
r	= yaw rate, rad/sec
λ	= eigenvalue
$\delta(\lambda(\sigma_{max}))$	= distribution of the eigenvalue with maximal real part
$\sigma(A)$	= minimum singular value of matrix A
$\bar{\sigma}(A)$	= maximum singular value of matrix A
τ	= effective time delay, sec
τ_p	= phase delay, sec
θ	= pitch angle, rad
ϕ	= roll angle, rad

Vectors

u	= control vector, $[\delta_{coll}, \delta_{lat}, \delta_{long}, \delta_{TR}]^T$
x	= state vector of rigid body states, $[u, v, w, p, q, r, \phi, \theta]^T$

Matrices

A	= open loop dynamics matrix
A^d	= desired closed loop dynamics matrix
B	= control distribution matrix
B^d	= desired control distribution matrix
$E(s)$	= multiplicative error matrix
$G(s)$	= open loop transfer matrix,
H	= feedforward gain matrix
$K(s)$	= compensator transfer matrix,
$K(s)G(s)$	= loop transfer matrix
K	= feedback gain matrix

Superscripts

d	= desired
T	= transposed
-1	= inverse

Subscripts

bw	= bandwidth
c	= commanded

Introduction

United States military rotorcraft handling quality specifications have been recently revised. The specifications are formulated as desired transfer functions between pilot inputs and vehicle outputs, i.e. attitude angles, attitude rates, or translational velocities [1].

Three desired response-types have been developed [1-2]. These are as follows:

1. Attitude Command with Attitude Hold (ACAH)
2. Rate Command with Attitude Hold (RCAH)
3. Translational Rate Command with Position Hold (TRCPH)

In ACAH, a constant control input must result in proportional attitude displacement. This response type is required for hover and low speed operations in conditions of degraded visual cueing and for divided attention tasks. In RCAH systems, attitude must diverge away from trim

for at least 4 seconds following a step command. This response type is preferred for fully attended operations in conditions of good visual cueing. For TRCPH, a constant controller force input must produce a constant translational rate and the rotorcraft must hold position if the force on the cockpit controller is zero. TRCPH is necessary to achieve Level 1 handling qualities in nap of the earth maneuvers in fair to poor visual cue environments.

Most unaugmented rotorcraft will not meet the new specifications and feedback control systems are necessary to improve handling qualities so that safe operation close to the earth in poor weather conditions and/or at night is possible. Since helicopter responses to control inputs are highly coupled, helicopter dynamics are characterized by multi-input-multi-output (MIMO) mathematical models and design of flight control systems for such vehicles is a true multivariable synthesis problem.

A modern four-bladed attack helicopter operating at low speed and hover is used to illustrate the flight control system design methodology. The dynamic response characteristics for this helicopter are typical of most high performance helicopters. Simulations and flight tests have shown that with such helicopter dynamics, even experienced helicopter pilots are unable to accomplish divided attention operations or relatively simple tasks in degraded visual environments. Handling qualities that minimize the involvement of the pilot in basic stabilization tasks are required to accomplish such operations. This requires a high bandwidth, multiply-redundant flight control system.

High bandwidth flight control systems require high bandwidth actuators [3], hence the rate and deflection limit characteristics of the actuators will impose significant limitations on the feedback gains. Additional factors that limit the maximum feedback gains are : (1) sensor noise amplification, (2) in-plane (lead-lag) rotor coupling and inflow dynamics [4], (3) phase-margin requirements and high frequency modeling uncertainty (rotor and structural flexure modes) and (4) the time delay due to digital implementation of the flight control laws [5-6].

This paper presents a method for control law design that will provide good command tracking, decoupling, gust attenuation, stability robustness, and meet proposed handling qualities specifications. The performance of the control law will be demonstrated by: (1) time and frequency responses, (2) unstructured singular value analysis and (3) stochastic root locus.

The control law structure consists of "inner" and "outer" feedback loops. This paper describes an eigenstructure methodology used to design inner loop control laws which decouple the vertical velocity, roll, pitch, and yaw rates. The resulting inner loop control laws provide integral response characteristics between pilot inputs and attitude angles and altitude.

Various command response types can then be achieved

by simple feedforward and feedback outer loops wrapped around the inner loops. Since the inner loop feedbacks are flight critical, redundancy will be required in these loops [7]. The outer loops are flight critical only under degraded flight conditions.

Desired Response Characteristics

The inner loop flight control system involves four channels. Vertical velocity, roll, pitch and yaw rates are the four sensor outputs (measurements) and collective pitch, cyclic lateral, cyclic longitudinal, and tail rotor collective pitch are the four actuator inputs. The linearized equations of motion for the helicopter at hover are:

$$\dot{x} = Ax + Bu$$

where A and B are given in Table 1.

A =

-0.02	-0.01	-0.01	-0.15	0.02	0.00	0	-0.67
-0.05	-0.05	-0.01	-0.03	-0.02	0.01	0.66	-0.00
-0.08	-0.07	-0.38	0.00	-0.00	0.04	0.02	0.01
0.46	-2.59	-0.18	-3.00	-0.53	0.42	0	0
0.37	0.19	-0.18	0.07	-0.59	0.00	0	0
1.09	0.73	-0.04	0.41	0.41	-0.49	0	0
0	0	0	1	0.00	-0.02	0	0
0	0	0	0	1	0.03	0	0

B =

-0.05	-0.01	0.47	-0.00
-0.04	0.28	0.01	0.36
-3.11	-0.00	0.01	0.00
-2.42	20.8	1.02	9.19
-0.32	0.25	-6.33	-0.06
5.79	-2.62	2.38	-11.1
0	0	0	0
0	0	0	0

Table 1 Open loop dynamics and control matrices

The open loop eigenvalues at hover are listed below in Table 2.

-3.2377 + .0000i	roll rate
.2110 ± .5296i	forward velocity
.0353 ± .7431i	side slip
-.9021 + .0000i	pitch rate
-.5695 + .0000i	yaw rate
-.3221 + .0000i	heave velocity

Table 2 Open Loop Eigenvalues

The open loop helicopter exhibits two undamped unstable modes in forward velocity and side slip. The doubling times for these modes are 19.5 seconds and 3.27 seconds respectively. Level 1 handling qualities specify minimum allowable time to double amplitude for low

frequency second order modes of 15 seconds [8-9]. Therefore the side slip response does not satisfy Level 1 handling qualities. Only the roll rate bandwidth is sufficiently high to guarantee good handling qualities.

The open loop frequency response of the helicopter at hover is shown in Fig. 1. It can be seen that there are two channels, roll and pitch, with singular values of 0.0006 and 0.006 at a frequency of 0.01 rad/sec. The closed loop tracking and gust attenuation will be very poor in these channels since the low frequency gains are so small.

Eigenstructure assignment is used to design the inner loop control laws so that the unstable responses are stabilized and decoupled, first order rate responses are achieved about each axis. The pole location associated with each rate response is selected to have sufficiently high bandwidth so that crisp response to command inputs is assured. The desired transfer functions between commands and inner loop regulated variables are given by

$$\frac{w}{w_c} = \frac{\lambda_w}{(s + \lambda_w)} \quad (1)$$

$$\frac{p}{p_c} = \frac{\lambda_p}{(s + \lambda_p)} \quad (2)$$

$$\frac{q}{q_c} = \frac{\lambda_q}{(s + \lambda_q)} \quad (3)$$

$$\frac{r}{r_c} = \frac{\lambda_r}{(s + \lambda_r)} \quad (4)$$

When the loops between the roll attitude and lateral command and pitch attitude and longitudinal command are closed, the response that the pilot sees will have integral characteristics. The high inner loop gain at low frequency provides good tracking of pitch and roll attitude commands and gust attenuation, while the roll off at high frequency helps to avoid potential instabilities due to high frequency rotor and structural dynamics. The desired transfer functions between forward velocity and pitch command and side velocity and roll command are

$$\frac{u(s)}{q_c(s)} = \frac{\lambda_q}{s(s + \lambda_u)} = \frac{\lambda_q}{s^2} \quad (5)$$

$$\frac{v(s)}{p_c(s)} = \frac{\lambda_p}{s(s + \lambda_v)} = \frac{\lambda_p}{s^2} \quad (6)$$

The eigenvalues λ_u and λ_v are associated with the linearized drag forces in the forward and side directions. Since the values of λ_u and λ_v are small, the transfer functions between lateral and longitudinal velocities and roll and pitch commands are essentially $\lambda_{p,q}/s^2$. Equations 1-6 are used to define the desired closed inner loop eigenstructure for the model.

Once the inner loop system has been designed to approximate the desired transfer functions given in Eqs. 1-6, various command response types can be achieved by simple single loop feedbacks or feedforwards.

The desired pitch and roll attitude transfer functions for ACAH are [1,3,10]

$$\frac{\phi}{\phi_c} = \frac{\omega_\phi^2}{(s^2 + 2\zeta\omega_\phi s + \omega_\phi^2)} \quad (7)$$

$$\frac{\theta}{\theta_c} = \frac{\omega_\theta^2}{(s^2 + 2\zeta\omega_\theta s + \omega_\theta^2)} \quad (8)$$

Similar second order transfer functions between forward and side velocity commands and outputs are desired for TRCPH. The inner loop control laws provide RCAH responses.

Control Law Design and Nominal Performance

Inner Loop Design

The theory of eigenstructure assignment is discussed in References 11 to 13. The feedback control law is assumed to be a linear function of the state vector

$$u = -Kx \quad (9)$$

and the feedback gain matrix, K, is selected such that this control law results in desired placement of the closed loop eigenvalues and shaping of the corresponding closed loop eigenvectors. The closed loop eigenvalues and eigenvectors must be specified by the designer. The ideal closed inner loop state equations for the helicopter model are derived from the desired transfer functions (Eqs. 1-6) as:

$$\dot{x} = A^d x + B^d x_c \quad (10)$$

where

$$A^d = \begin{vmatrix} -\lambda_u & 0 & 0 & 0 & 1 & 0 & 0 & \lambda_q \\ 0 & -\lambda_v & 0 & 1 & 0 & 0 & \lambda_p & 0 \\ 0 & 0 & -\lambda_w & 0 & 0 & 0 & 0 & 0 \\ 0 & 0 & 0 & -\lambda_p & 0 & 0 & 0 & 0 \\ 0 & 0 & 0 & 0 & -\lambda_q & 0 & 0 & 0 \\ 0 & 0 & 0 & 0 & 0 & -\lambda_r & 0 & 0 \\ 0 & 0 & 0 & 1 & 0 & 0 & 0 & 0 \\ 0 & 0 & 0 & 0 & 1 & 0 & 0 & 0 \end{vmatrix}$$

$$B^d = \begin{bmatrix} 0 & 0 & 0 & 0 \\ 0 & 0 & 0 & 0 \\ \lambda_w & 0 & 0 & 0 \\ 0 & \lambda_p & 0 & 0 \\ 0 & 0 & \lambda_q & 0 \\ 0 & 0 & 0 & \lambda_r \\ 0 & 0 & 0 & 0 \\ 0 & 0 & 0 & 0 \end{bmatrix}$$

The values of $\lambda_{w,p,q,r}$ for the ideal A matrix are determined from the handling qualities requirements. A bandwidth of 4 rad/s for vertical velocity, roll, pitch and yaw rate was chosen to assure Level 1 handling qualities. Based on previous experience, the values of λ_u and λ_v were selected to be -.00199 and -.00526, 10% of their nominal values. With the closed loop eigenvalues specified, A^d is then used to define the desired eigenvalue/eigenvector configurations. This configuration is achieved in a best least square sense using eigenstructure assignment.

The extensive coupling of the control distribution matrix, B, requires a feedforward gain matrix to alleviate the problem of control cross-coupling. The feedforward gain matrix, H, was selected such that

$$B * H \approx B^d \quad (11)$$

Since the control distribution matrix B is non-square, it is necessary to solve for H using the pseudo-inverse method [14], which is optimal in the sense that $\text{tr}(B^T * B)(B^T * B)$ is minimized. Solving for H yields

$$H = (B^T * B)^{-1} * B^T * B^d \quad (12)$$

This result achieves the decoupling desired for the four control inputs. It also includes some unwanted input dynamics in forward and side velocities for heave command, forward velocity for longitudinal command, and side velocity for yaw rate command. Although these coupling terms are undesirable, they are tolerable since their magnitudes are small.

Figure 2 shows the singular value plot of the identity matrix minus the inner closed loop transfer function matrix between commands and rates. For a system to have good decoupling characteristics, the $\bar{\sigma}[I - G_{\text{closed loop}}]$ must be smaller than unity in the frequency range of interest. As shown in Fig. 2, decoupling of the heave mode is not achieved at low frequencies but the controller has been able to achieve small gains over frequency range of interest, 0.1 to 10 rad/sec, in each of the four control channels. The coupling at low frequencies results because of incomplete pole/ zero cancellation.

A plot of the transfer function response of the three components of the accelerations of the center of gravity to a vertical gust is shown in Fig. 3. As expected, longitudinal and lateral accelerations are insensitive to a vertical gust. The small singular values at low frequencies [15] show good attenuation of vertical acceleration. The vertical acceleration has a bandwidth of 4 rad/sec. Even at frequencies above the bandwidth, the gain between vertical acceleration and vertical gust is only 0.4. Although no specifications exist for gust response, Key [2] indicates that the bandwidth of the gust should be about the same as the bandwidth of command response to ensure adequate disturbance rejection.

The full state regulator in the inner loop requires that all states be fed back. Since only vertical velocity, pitch rate, roll rate and yaw rate are measured in the inner loop, it is necessary to include a state estimator in the feedback loop in order to implement the control law.

The estimator gain is chosen such that the estimator is stable and the frequency response of the system with the regulator/estimator in the feedback loop approximates that for full state loop transfer matrix. This is called loop transfer recovery (LTR). The details of LTR using eigenstructure assignment are given in Reference 16.

Outer Loop Design

Once the inner loop system has been designed to approximate the desired transfer functions given in Equations 1 to 6, various command response types can be achieved by simple single loop feedback or feedforward loops. The design of an ACAH system will be used to illustrate the method.

The lateral and longitudinal angles, ϕ and θ , can be fed back by an outer loop with a proportional gain of K_ϕ and K_θ to achieve ACAH. Thus only the roll and pitch angle measurements are needed for the outer loop design. The resulting transfer functions between commanded and actual pitch and roll angle are given in Eqs. 13 to 14. Both K_ϕ and K_θ were selected as 2. The transfer functions are second order with a natural frequency, $\omega_{n\phi,\theta} = 2.83$ rad/sec and a damping ratio, $\zeta = 0.707$

$$\frac{\phi}{\phi_c} = \frac{K_\phi \lambda_p}{(s^2 + \lambda_p s + 2\lambda_p)} \quad (13)$$

$$\frac{\theta}{\theta_c} = \frac{K_\theta \lambda_q}{(s^2 + \lambda_q s + 2\lambda_q)} \quad (14)$$

Using the handling quality specification for a second order system, the desired bandwidth is defined in terms of the natural frequency and damping ratio of the system as in Eq. 15. This type of bandwidth is phase margin limited and is defined as the frequency where the phase angle becomes -135. The roll and pitch attitude

command response give Level 1 handling qualities with a bandwidth of 5.46 rad/sec.

$$\omega_{bw} = \omega_n (\zeta + \sqrt{\zeta^2 + 1}) \quad (15)$$

The eigenvalues corresponding to the vertical velocity mode, the roll and pitch attitudes modes, and the yaw rate mode were as specified. There was a low frequency, oscillatory mode with a frequency of $\omega = 0.014$ rad/s and a damping ratio of $\zeta = 0.043$.

The decoupled character of the response is further illustrated in Fig. 4 which shows the response to a 5 deg roll angle command which is maintained for four seconds and then returned to zero. The results were plotted such that all linear velocities and angular displacements are on the same graphs to better illustrate the closed loop decoupling. The response of the side velocity to roll command results in an acceleration command/ velocity hold type of response. Once the attitude achieves its commanded value, the control is returned to the zero stick position. The attitude drops back to its original value within two seconds after the control is released, whereas, the side velocity remains almost constant. Fig. 4 also shows that after the stick has been released, there is a slight increase in the forward velocity. Pitch attitude remains unchanged at zero through out the 10 seconds indicating that the decoupling is good.

Closed outer loop time responses were also calculated for a 5 ft/sec step command in vertical velocity. Pilot collective and pedal commands are of primary importance in maintaining hover. Considerable training and coordination are required for pilots to maintain a helicopter at a constant altitude during hover. Decoupling response to collective and pedal inputs results in improved handling qualities. Figure 5 illustrates the response to a collective input from the pilot. A collective pitch change from the pilot input gives a change in the mean blade angle of attack, which produces a change in the thrust magnitude. The change in thrust magnitude increases the main rotor torque, which in turn requires the increase in the tail rotor thrust power to provide the anti-torque forces to balance the helicopter. There is a non negligible side velocity which is caused by the change in tail rotor pitch required to balance the main rotor torque. Fig. 5 shows that the side velocity increases linearly in order to keep a constant yaw rate. Correction of this side velocity would require a small lateral stick input. It can be seen that the yaw rate, roll rate, and pitch rate are all negligible. Figure 6 shows the effect of a step yaw rate command of 5 deg/sec. The change in vertical velocity is negligible; however the lateral and longitudinal responses are small but not negligible and would require both lateral and longitudinal stick inputs for stabilization. During yawing maneuvers, the drag force of a tail rotor must be countered by the main rotor. The decoupling of all states is improved when the outer loop is closed.

Since pilots are sensitive to the shape of the phase curve at frequencies above the bandwidth frequency, phase

delay parameter, τ_p as defined in Eq. 16 is used for the evaluation of the design.

$$\tau_p = \frac{\Delta\Phi 2\omega_{180}}{57.3 (2\omega_{180})} \quad (16)$$

For large values of phase delay, the phase curve drops off more rapidly than for small values [2]. The evaluation of τ_p is based on the assumption that the ACAH system has a total effective time delay of 0.15 sec. The resulting bode magnitude and phase plots about the roll axis of the ACAH system plus total effective time delay is shown in Figure 7. From Figure 7, $\Delta\Phi 2\omega_{180}$ is determined to be 57.57 deg and $2\omega_{180}$ is determined to be 10.98 rad/sec. Using Eq. 16, the phase delay of the overall system is calculated to be $\tau_p = 0.092$ sec. As shown in Fig. 8, this value satisfies Level 1 handling quality requirements for ultra high gain tasks.

Stability Robustness

Unstructured Singular Value Analysis

Since the inner loop system is flight critical, the stability robustness of this system with respect to modeling errors and parameter variations is very important. An error model which gives an approximation of the high frequency modeling uncertainties is developed. This error model approximates the unmodeled high frequency dynamics of structural modes, actuators, filters, sensors, sampling delays, and computational delays associated with digital implementation of the flight control system with effective time delays. The total effective time delays for each of the four input channels is assumed to be the same. Additional assumptions are: (1) there is no cross-coupling of the uncertainties between channels, and (2) the nominal model has a 10% error at low frequencies.

The multiplicative error model, given by Eq. 17 is utilized in the stability robustness test. The multiplicative error matrix is defined as

$$G_{true}(s) = G(s)(I + E(s)) \quad (17)$$

and is related to the effective time delay, $\Delta\tau$ by the following equation [6],

$$I + E(s) = \text{diag}\{ e^{-s\Delta\tau} \} \quad (18)$$

Using a first order Pade approximation for the total effective time delay, the error can then be evaluated as

$$E(s) = \left(\frac{-2\Delta\tau s}{\Delta\tau s + 2} \right) I \quad (19)$$

A sufficient condition [17] for the closed inner loop system to be robustly stable with respect to $E(s)$ is

$$\underline{\sigma} (I + [K(s)G(s)]^{-1}) > \bar{\sigma} (E(s)) \quad \forall s = j\omega \quad (20)$$

where $0 < \omega < \infty$.

Element	Delay (msec)
Rotor	66
Actuators	31
Zero-order hold	17
Computations	22
Notch filter	11
Total delay	147

Table 3 Summary of Time Delay Contributors.

Many components of the effective time delay such as delays due to rotor response and structural dynamics are essentially fixed; however, others such as computational delays and sampling times may be influenced by the design of the flight control system hardware and software. For example, a faster computer, more effective computational algorithms, or a faster sampling rate may be used to reduce control system delays. Based on the data in Reference 10, a break down of the various delays is given in Table 3. The total effective time delay is chosen to be 0.15 sec. The modeling error is estimated to lie within the shaded region shown in Fig. 9. If the modeling error is indeed within this region, stability of the closed loop system is assured if Eq. 20 is satisfied.

As can be seen in Fig. 9, the frequency at which the condition given in Eq. 20 fails is below 0.01 rad/sec. The condition given by Eq. 20 is conservative and the helicopter may not be unstable. Furthermore the frequency of 0.01 rad/sec is much lower than the 4 rad/sec bandwidth of the closed inner loop system and if the helicopter exhibits instabilities at these low frequencies, it may not have any significant effect on the handling qualities.

Figure 9 illustrates that the stability robustness of the helicopter is further improved when the outer loop is closed. With the outer loop closed, the integral character of roll and pitch attitudes becomes a second order. As a result, closing the outer loop improves the stability robustness of the system at frequencies below 0.01 rad/sec. A measure of the robustness of a MIMO system is the smallest difference between the minimum singular value of $[I + K(s)G(s)]^{-1}$ and the maximum singular value of the multiplicative error, $E(s)$. This can be regarded as a MIMO gain margin. As shown in Fig. 9, the minimum difference between the two curves is 6.7 dB at about 7.39 rad/sec.

Stochastic Root Locus

Since the unstructured singular value analysis indicated a possible low frequency instability, it is necessary to examine in detail the effects of modelling errors due to variations in the aerodynamic stability and control derivatives. This can be accomplished by the use of the

stochastic root locus where one or more parameters are changed at random. The stochastic root locus is similar to the usual root locus where a parameter is varied in a continuous way. The stochastic root locus gives a distribution of the eigenvalues in the s-plane.

The main purpose of doing this kind of a root locus is to decide whether the system is stable or unstable, and if the system is unstable, to estimate the degree of instability.

The stochastic root locus is a three dimensional plot with the s-plane horizontal and the distribution of the eigenvalues in the vertical direction. The construction of such a plot is described by Stengel and Ryan [18]. The s-plane is divided in "infinitesimal" rectangles, which they call "bins". If a eigenvalue is found that fits in this bin then it is stacked to the "pile" related to it.

The height of the surface created with respect to the s-plane gives a measure of the likelihood of encountering an eigenvalue in that region. This procedure gives a very good idea of the behavior of the system if there are a large number of parameter uncertainties. The resultant root locus is shown in Figs. 10 and 11. Fig. 10 shows the three dimensional plot and Fig. 11 shows the distribution of the real part of the eigenvalue with maximum real part.

The stochastic root locus shows that the inner loop system is mainly unstable under $\pm 20\%$ variations of the elements in A and B which depend on the aero-coefficients. But this instability is tolerable if it is occurs within certain limits.

According to [9] for Level 2 handling qualities, the largest positive real part of the eigenvalue is 0.139. This value lies above the mean value of the stochastic evaluations (see Fig. 11). The inner loop system meets the Level 2 handling quality with a probability lying in the interval [59.6%, 61.6%] with a 95% confidence.

There is still roughly a 40% chance that the closed loop system is unstable and does not meet Level 2 handling qualities.

For the worst case ($\sigma_{\max} = 0.3973$) achieved in these statistical evaluations the closed loop system has the following eigenvalues:

$$\underline{\lambda}_{\text{woc}} =$$

0.3973
0.1061
-0.1212
-0.4628
-3.5821
-3.7563
-4.0327
-4.2398

The high frequency bandwidth, which was specified as

4 rad/s in all channels, is still acceptable. The largest unstable eigenvalue would result in a doubling time of 1.75 sec (minimum doubling time for Level 2 handling qualities is 5 sec). Thus in the worst case, the handling qualities of the helicopter would be poor. On the other hand as seen from Figs. 10 and 11 the probability of such an event is small and there is a 60% chance that Level 2 or better handling qualities will exist under a $\pm 20\%$ random variation in the aerodynamic coefficients.

Conclusions

The methodology described in this paper provides a straight forward approach to the design of helicopter flight control systems which provide response types necessary to meet new handling quality specifications. The control laws provide excellent response to pilot and commands, gust attenuation and acceptable stability robustness. Control laws are of relatively low order and implementation should be relatively simple.

Acknowledgement

This research was supported by the U.S. Army Research Office under Contract DAAL03-86-K-0056.

References

1. Hoh, R. H., "Dynamics Requirements in the New Handling Qualities Specification for US Military Rotorcraft," Proceedings of Royal Aeronautical Society International Conference on Helicopter Handling Qualities and Control, London, Nov. 1988.
2. Key, David L., "A New Handling Qualities specification for U.S. Military Rotorcraft," Proceedings of Royal Aeronautical Society International Conference on Helicopter Handling Qualities and Control, London, Nov. 1988.
3. Tischler, Mark B., "Assessment of Digital Flight-Control Technology for Advanced Combat Rotorcraft," *Journal of the American Helicopter Society*, Oct. 1989, pp 66-76.
4. Miller, D. G. and White, F., "A Treatment of the Impact of Rotor-Fuselage Coupling on Helicopter Handling-Qualities," 43rd Annual National Forum of the American Helicopter Society, May 1987.
5. Smith, Roger E. and Sarrafian, Shahan K., "Effect of Time Delay on Flying Qualities: An Update," *Journal of Guidance, Control and Dynamics*, Vol. 9, No. 5, Sept.- Oct. 1986, pp 578-584.
6. McRuer, D. T., Myers, T. T., Thompson, P. M., "Literal Singular-Value-Based Flight Control System Design Techniques," *Journal of Guidance, Control and Dynamics*, Vol. 12, No. 6, Nov.- Dec. 1989, pp 913-919.
7. Hendrick, Russell C., "Flight Controls for Advanced Military Helicopters," *Scientific Honeyweller*, pp 144-152, Winter 1989.
8. Hoh, R. H., Mitchell, D. G., Aponso, B. L., Key, D. L., and Blanken, C. L., "Proposed specification for Handling Qualities of Military Rotorcraft, Vol. 1 - Requirements," U.S. Army Aviation Systems Command, Moffett Field, CA, TR-87-A-4, May 1988.
9. Aponso, Bimal L., Mitchell, David G. and Hoh, Roger H., "Simulation Investigation of the Effects of Helicopter Hovering Dynamics on Pilot Performance," *Journal of Guidance, Control and Dynamics*, Vol. 13, No. 1, Jan.- Feb. 1990, pp 8-15.
10. Tischler, Mark B., Fletcher, Jay W., Morris, Patrick M., and George, T. Tucker, "Application of Flight Control System Methods to an Advanced Combat Rotorcraft," Proceedings of Royal Aeronautical Society International Conference on Helicopter Handling Qualities and Control, London, Nov. 1988.
11. Cunningham, Thomas B., "Eigenspace Procedures for Closed Loop Response Shaping with Modal Control," Proceedings 19th IEEE Conference on Decision and Control, Dec. 1980, pp 178-186.
12. Andry, A. N., Shapiro, E. Y., and Chung, J.C., "Eigenstructure Assignment for Linear Systems," *IEEE Trans. on Aerospace Electronic Systems*, Sept. 1983, Vol. AES-19, pp 711-729.
13. Sobel, K. M. and Shapiro, E. Y., "Eigenstructure Assignment : A Tutorial - Part 1 Theory," Proceeding of the 1985 ACC, Boston, MA, June 1985, pp 456-460.
14. Strang, Gilbert, *Linear Algebra and its Applications*, 3rd Edition, Harcourt Brace Jovanovich, Publishers, San Diego, 1988.
15. Baillie, Stewart W., Morgan, J. Murray, "Control Sensitivity, Bandwidth and Disturbance Rejection Concerns for Advanced Rotorcraft," Presented at the 45th Annual Forum of the American Helicopter Society, Boston, Massachusetts, 22-24 May, 1989.
16. Kazerooni, H., and Houpt, P. K., "On the Loop Transfer Recovery," *Int. Journal of Control*, Vol 43, 1986, pp 981-996.
17. Lehtomaki, N. A., Sandell, N. R., and Athans, M., "Robustness Results in Linear Quadratic Based Multivariable Controller Design," *IEEE Trans. on Auto. Control*, Vol 26, Feb 1981, pp 75-92.

18. Stengel, R. F., and Ryan, L. E., "Stochastic Robustness of Linear Control Systems", *Proceedings of 1989 Conference on Information Sciences and Systems, John Hopkins University, Baltimore, March 1989*

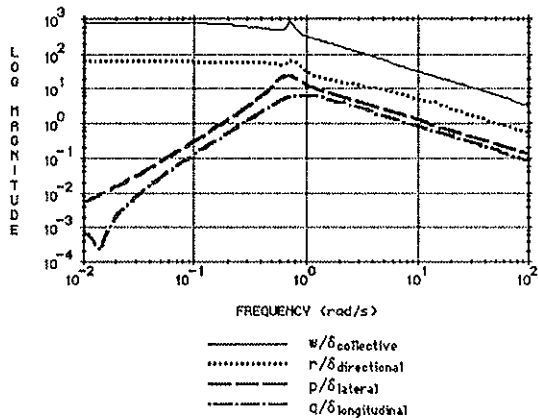


Fig. 1 Singular Value Plot of Open Loop Helicopter at Hover

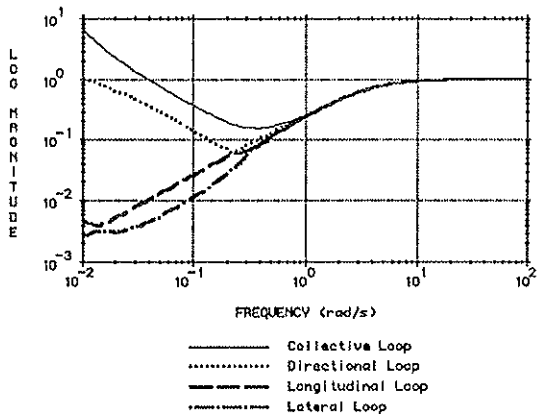


Fig. 2 Singular Values of $[I-G_{Closed Inner Loop}]$

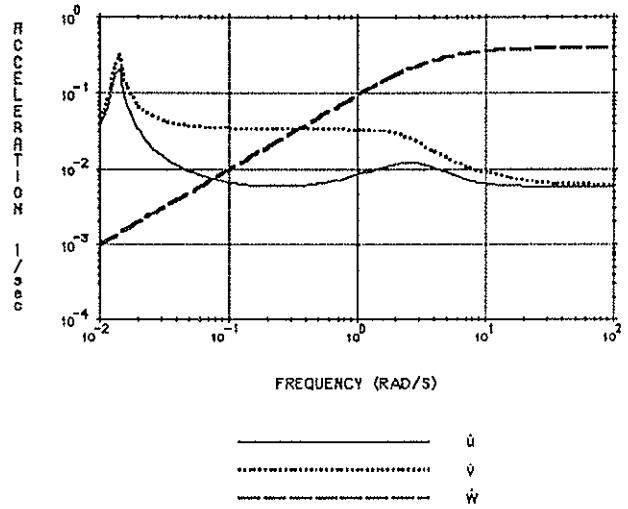


Fig. 3 Full State Closed Inner Loop Response of Accelerations to Vertical Gust

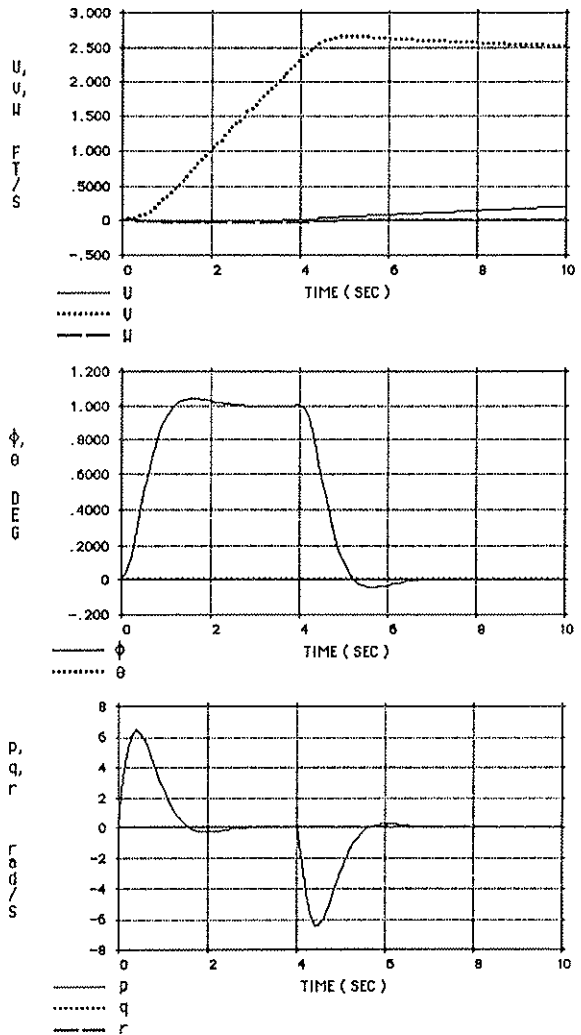


Fig. 4 Full State Closed Outer Loop Response to a 5° Step Roll Command of 4 sec Duration

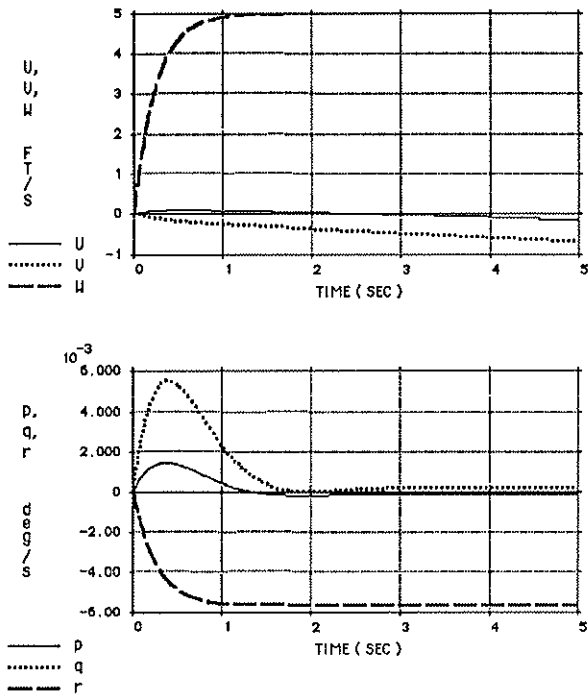


Fig. 5 Full State Closed Outer Loop Response to a 5 ft/sec Heave Command

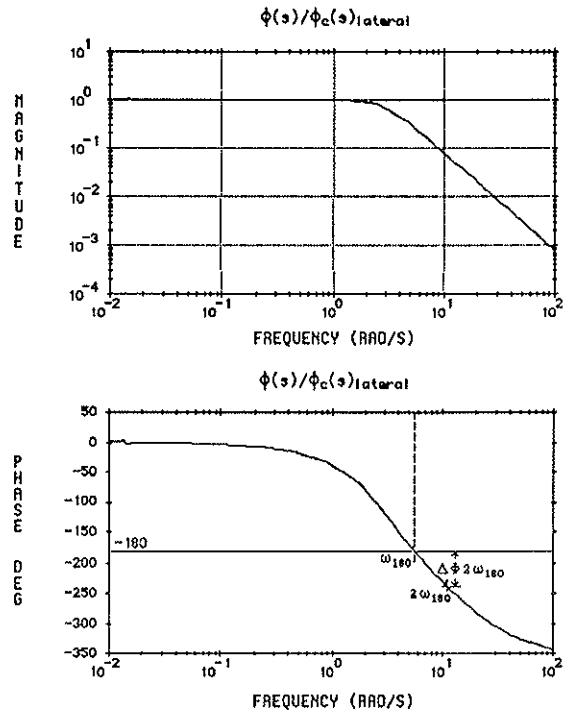


Fig. 7 Frequency Response of Closed Loop Roll Attitude with Effective Time Delay Included

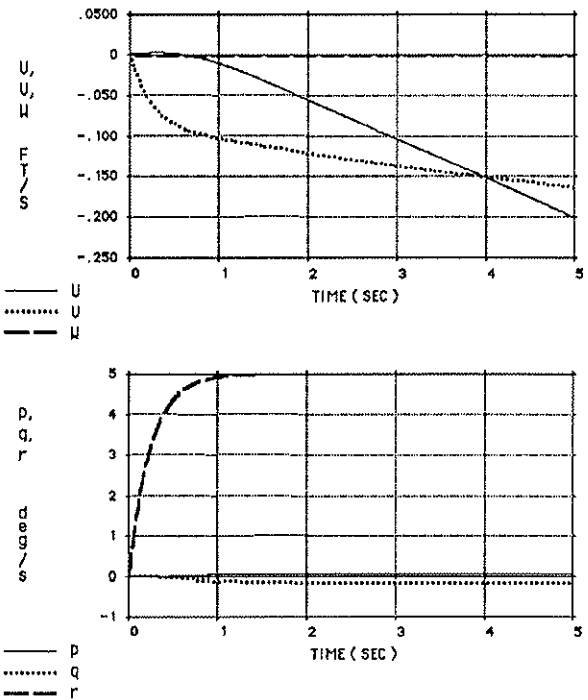


Fig. 6 Full State Closed Outer Loop Response to a 5 ft/sec Yaw Rate Command

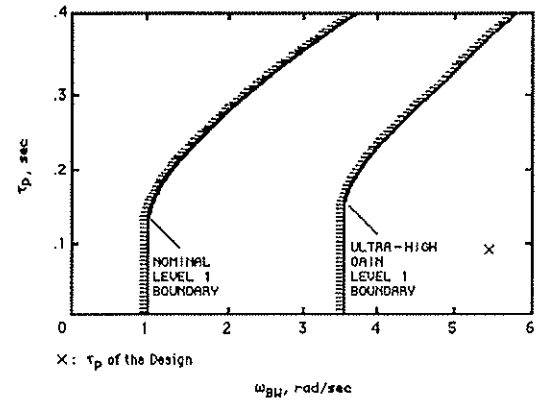


Fig. 8 Level 1 Small-Amplitude Requirements for Minimum and Maximum Gain Tasks

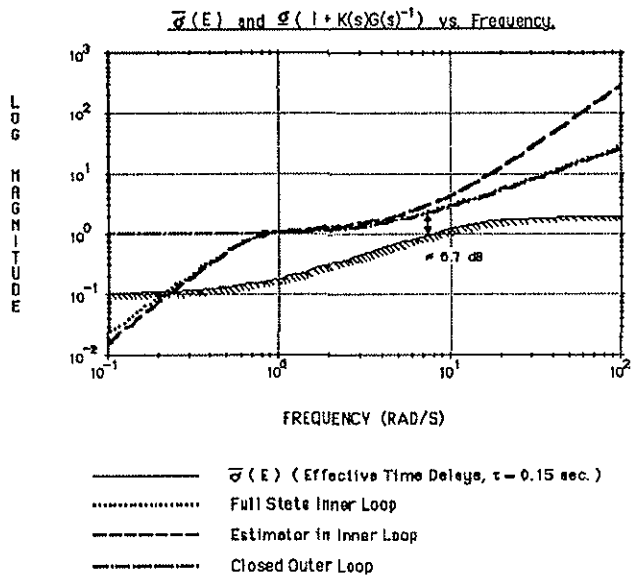


Fig. 9 Minimum Singular Values for Full State Closed Inner and Outer Loops, Estimator in the Feedback Loop and Maximum Singular Values of Error Matrix vs. Frequency

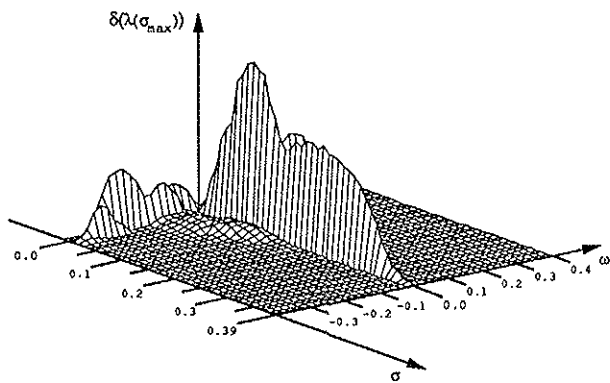


Fig. 10 Distribution of the Eigenvalue With the Maximum Real Part (25,000 iterations)

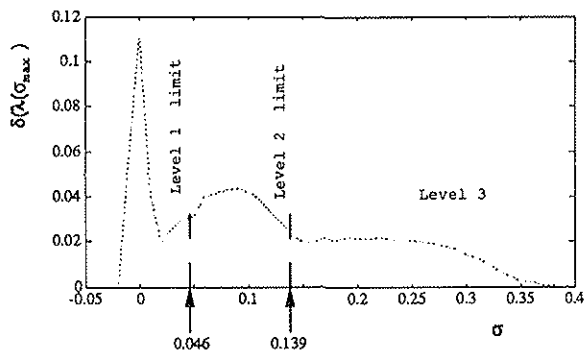


Fig. 11 Distribution of the Real Part of the Eigenvalue With Maximum Real Part